



HAL
open science

A computationally effective dynamic hysteresis model taking into account skin effect in magnetic laminations

Olivier de La Barrière, Carlo Ragusa, Carlo Appino, Fausto Fiorillo, Martino Lobue, Frederic Mazaleyrat

► **To cite this version:**

Olivier de La Barrière, Carlo Ragusa, Carlo Appino, Fausto Fiorillo, Martino Lobue, et al.. A computationally effective dynamic hysteresis model taking into account skin effect in magnetic laminations. *Physica B+C*, 2014, 435, pp.80 - 83. 10.1016/j.physb.2013.09.036 . hal-01100311

HAL Id: hal-01100311

<https://hal.science/hal-01100311v1>

Submitted on 8 Jan 2015

HAL is a multi-disciplinary open access archive for the deposit and dissemination of scientific research documents, whether they are published or not. The documents may come from teaching and research institutions in France or abroad, or from public or private research centers.

L'archive ouverte pluridisciplinaire **HAL**, est destinée au dépôt et à la diffusion de documents scientifiques de niveau recherche, publiés ou non, émanant des établissements d'enseignement et de recherche français ou étrangers, des laboratoires publics ou privés.

A computationally effective dynamic hysteresis model taking into account skin effect in magnetic laminations

O. de la Barrière¹, C. Ragusa², C. Appino³, F. Fiorillo³, M. LoBue¹, F. Mazaleyrat¹

¹ SATIE, ENS Cachan, CNRS, UniverSud, 61 av du Président Wilson, Cachan, France.

² Dip. Energia, Politecnico di Torino, C.so Duca degli Abruzzi 24, 10129 Torino, Italy.

³ Istituto Nazionale di Ricerca Metrologica (INRIM), Torino, Italy.

2 **Abstract**

3 We propose a simplified dynamic hysteresis model for the prediction of magnetization behavior of
4 electrical steel up to high frequencies, taking into account the skin effect. This model has the advantage
5 of predicting the hysteresis loop and loss behavior versus frequency with the same accuracy provided
6 by the Dynamic Preisach Model with a largely reduced computational burden. It is here compared to
7 experimental results obtained in Fe-Si laminations under sinusoidal flux up to 2 kHz.

8

9 I. INTRODUCTION

10 The problem of high frequency behavior of magnetic laminations is of primary importance in
11 modern electrical engineering problems [1], but difficult problems arise in the prediction and
12 assessment of magnetization process and losses, because the skin effect compounds with the nonlinear
13 hysteretic response of the material. In order to cope with the inhomogeneous profile of the flux density
14 over the lamination thickness, the magnetic loss is generally calculated by numerically solving the
15 diffusion equation over the sample cross-section, and using a dynamic hysteresis model for the material
16 constitutive law [2]. The Dynamic Preisach Model (DPM) is the model of choice, because it is accurate
17 and solidly established from the physical viewpoint [3][4]. Its application is, however, particularly time
18 consuming, because calculations must be done for each finite element of the spatial mesh until
19 convergence is reached. A faster approach, preserving the special virtues of DPM, would therefore be
20 appropriate. We apply in this paper the DPM to the broadband behavior of nonoriented Fe-Si
21 laminations through a simplified method, drastically reducing computing time and complexity of the
22 full method, requiring the computation of the dynamics of each elementary hysteron distributed in the
23 Preisach plane [5]. We start our discussion from the differential relation found by Bertotti [6] (formula
24 (9), page 4609, of reference [6]) for the excess magnetic field due to the dynamic behavior of the
25 magnetization process

$$H_{\text{exc}}(t) \equiv H(t) - H_{\text{stat}}(t) = \text{sign}(\dot{H}_{\text{stat}}) \frac{4}{3} \sqrt{\frac{|\dot{H}|}{k_d}}, \quad (1)$$

26 where $H(t) = H_a(t) - H_{\text{cl}}(t)$ is the difference between the applied field $H_a(t)$ and the counterfield $H_{\text{cl}}(t)$
27 generated by the macroscopic eddy currents (classical field). $H_{\text{stat}}(t)$ is the field that would provide
28 under static conditions the same irreversible polarization J_{irr} and k_d [$\text{A}^{-1}\text{s}^{-1}\text{m}$] is the DPM constant. Eq.
29 (1) is derived under the simplifying assumptions of triangular $H_a(t)$ and uniform Preisach distribution
30 function. The extent to which such a restriction can be circumvented and the full DPM approach for

31 generic exciting conditions and shape of the Preisach density function can be approximated will be
 32 discussed in the following. We find first that a numerical analysis based on (1) (Model 1) does not lead
 33 to highly accurate dynamic loop shapes, especially at high frequencies. A slight modification of (1) is
 34 therefore proposed (Model 2) and implemented in a non-linear magneto-dynamical model for the
 35 computation of the field distribution inside Fe-Si laminations, taking into account skin effect. The
 36 numerical results are compared with the experiments performed under sinusoidal flux up to 2 kHz.

37 II. THE SIMPLIFIED MODEL

38 A. The simplified DPM-Model 2

39 The Preisach distribution function, including the reversible contribution, was determined in a 0.35
 40 mm thick Fe-(3.2wt%)Si-(0.5wt%)Al lamination, and the dynamic constant $k_d=350 \text{ A}^{-1}\text{s}^{-1}\text{m}$ was
 41 identified. The full and the simplified (Model 1) DPM are compared in terms of the excess field. In this
 42 model benchmark, a sinusoidal dynamic field $H(t) = H_a(t) - H_{cl}(t)$ (peak value $H_p = 100\text{A}\cdot\text{m}^{-1}$,
 43 frequency $f = 200 \text{ Hz}$) has been applied. For the full DPM case, the excess field $H_{\text{exc}}(t) = H(t) - H_{\text{stat}}(t)$
 44 is derived applying the DPM to $H(t)$ in order to get the irreversible polarization $J_{\text{irr}}(t)$, and then using
 45 the inverse static Preisach model to compute the static field $H_{\text{stat}}(t)$ from $J_{\text{irr}}(t)$. For the model 1, a
 46 numerical solution of (1) directly provides $H_{\text{stat}}(t)$ from the sinusoidal $H(t)$. A comparison between the
 47 results of two approaches is illustrated in Fig. 1 (the J_{irr} waveform obtained from the DPM has also
 48 been represented). Discrepancies are found between the two predicted $H_{\text{exc}}(t)$ waveforms, particularly
 49 around the reversal points of the irreversible magnetization J_{irr} . With the simplified Model 1 the zero of
 50 H_{exc} is, according to (1), coincident with the maximum of $H(t)$, whereas from the same picture, it
 51 appears that it occurs when J_{irr} is maximum. Consequently, (1) is formulated as

$$H_{\text{exc}}(t) \equiv H(t) - H_{\text{stat}}(t) = \text{sign}(\dot{H}_{\text{stat}}) \frac{4}{3} \sqrt{\frac{|\dot{H}_{\text{stat}}|}{k_d}}, \quad (2)$$

52 on account of the fact that the sign of \dot{H}_{stat} is the same as that of \dot{J}_{irr} . The simplified DPM based on

53 (2) (DPM-Model 2) appears now to provide (Fig. 1) an $H_{\text{exc}}(t)$ waveform in good agreement with the
 54 one provided by the full DPM.

55 Once the static field is known, $J_{\text{irr}}(H_{\text{stat}})$ is computed by means of the Static Preisach Model, while
 56 the reversible component $J_{\text{rev}}(H)$ is calculated ignoring any dynamic effect linked to the reversible
 57 contribution [1]. This procedure, which permits to obtain the constitutive law of the material $J(H)$, is
 58 summed up in Fig. 2. An example of hysteresis loop prediction (in this case with nested minor loop) is
 59 illustrated in Fig. 3, confirming the good agreement between the results provided by the full DPM and
 60 the simplified DPM-Model 2.

61 A. Numerical implementation of DPM-Model 2

62 This model requires solving the non-linear differential equation (2) for H_{stat} knowing the field H .
 63 This can be done putting (2) under an equivalent canonical form and adding the periodicity conditions
 64 (period $T=1/f$):

$$\begin{cases} \dot{H}_{\text{stat}} = \text{sign}(H(t) - H_{\text{stat}}(t)) \cdot \frac{9k_d}{16} \cdot (H(t) - H_{\text{stat}}(t))^2 \\ H_{\text{stat}}(0) = H_{\text{stat}}(T) \end{cases} \quad (3)$$

65 and numerically solving it using a Runge-Kutta method. The application of this newly defined
 66 dynamical model to the computation of flux distribution inside the steel lamination can dramatically
 67 reduce the computational burden, as demonstrated in the next section.

68 III. MAGNETO DYNAMICAL MODELING AND EXPERIMENTAL

69 A. Magneto-dynamical model of the lamination

70 The solution of the diffusion equation over the lamination thickness with a dynamic hysteretic
 71 constitutive law requires a special numerical treatment of the non-linearity using the Fixed Point
 72 method [3][7]. The method proposed in [3] has been here implemented. The diffusion problem on the
 73 lamination thickness is one-dimensional, with the spatial coordinate x ranging over the lamination

74 cross-section $[-e/2; e/2]$ (where $e = 0.35$ mm is the lamination thickness). To solve the diffusion
 75 equation, the non-linearity of the material constitutive law $J(H)$ is contained in a spatio-temporal
 76 function $R(x,t)$, called the residual [3] and the relationship between H and J is written as

$$H(x,t) = v_{\text{FP}} \cdot B(x,t) + R(x,t), \quad (4)$$

77 where v_{FP} is a properly chosen constant, ensuring convergence [1]. Using (4), the diffusion equation
 78 can be written, with imposed mean flux density $B_{\text{MEAN}}(t)$, in terms of vector potential A on a half
 79 lamination $[0; e/2]$:

$$\begin{cases} v_{\text{FP}} \cdot \frac{\partial^2 A}{\partial x^2} - \sigma \frac{\partial A}{\partial t} = \frac{\partial R}{\partial x} \\ A(0,t) = 0 \text{ and } A(e/2,t) = -B_{\text{MEAN}}(t) \cdot e/2 \\ A(x,t) \text{ is } T\text{-periodic} \end{cases} \quad (5)$$

80 The time derivative and the time periodic condition are dealt with using temporal Fourier series [3].
 81 More precisely, the residual function $R(x,t)$ is decomposed into complex Fourier series for what
 82 concerns the time dependence. Equation (5) is then solved for each time harmonic, the time derivative
 83 becoming an algebraic multiplication by the corresponding harmonic pulsation. An inverse Fourier
 84 transformation permits to retrieve the function $A(x,t)$. For each time harmonic, the spatial second order
 85 derivative and the boundary conditions are dealt with using a numerical finite difference scheme (the
 86 half lamination is subdivided into 50 intervals). At the beginning of the iterative procedure, the residual
 87 R is initialized to zero and at each iteration step (index number i), the following process is performed:

88 1. Knowing the residual at the previous stage $R^{(i-1)}(x,t)$, the differential equation (5) is solved to
 89 compute the vector potential $A^{(i)}(x,t)$. The magnetic field is obtained as

$$90 \quad H^{(i)}(x,t) = -v_{\text{FP}} \frac{\partial A^{(i)}}{\partial x} + R^{(i-1)}(x,t).$$

91 2. A dynamic hysteresis model, providing the dynamic constitutive law $J(H)$, is used to evaluate $J^{(i)}$

92 from $H^{(i)}$ and the new induction value $B^{(i)}(x,t)=J^{(i)}(x,t)+\mu_0\cdot H^{(i)}(x,t)$ is calculated. In [3], the dynamic
 93 hysteresis model is the DPM, and is replaced in this paper by the simplified model proposed in Fig.
 94 2.

95 3. The new residual is then computed by $R^{(i)}(x,t)=H^{(i)}(x,t)-v_{FP}\cdot B^{(i)}(x,t)$. The process is repeated
 96 until convergence of the residuals is obtained.

97 B. Results

98 The dynamic hysteretic constitutive law $J(H)$ of the material, which was in [3] given by the full
 99 DPM, has been here replaced by the model proposed in Fig. 2 where the Model 2 of the local excess
 100 field is applied. The Preisach distribution function has been identified following the method proposed
 101 in [1], in the previous 0.35 mm thick Fe-(3.2wt%)Si-(0.5wt%)Al lamination (conductivity $\sigma =$
 102 $1.773\cdot 10^6 \text{ S}\cdot\text{m}^{-1}$, $k_d=350 \text{ A}^{-1}\text{s}^{-1}\text{m}$). The magnetic loss and hysteresis loops have been measured under
 103 sinusoidal flux at different frequencies and peak inductions up to 2 kHz. The magnetic flux distribution
 104 and loss have been computed by applying the dynamical model, using both the full and the simplified
 105 DPM (Model 2). Fig. 4 provides an example of computed and experimental loops ($J_p = 0.5 \text{ T}$,
 106 frequency $f = 1 \text{ kHz}$). In Fig. 5 the comparison is made for energy loss versus frequency behavior. It
 107 shows the good predicting capability of the simplified dynamic Model 2, in spite of a computing time
 108 reduced by a factor around 60 with respect to the full DPM. Fig. 5 also shows the predicted loss
 109 behavior if the skin effect is ignored. In this case the induction is assumed uniform across the sample
 110 thickness and equal to the mean flux density $B_{\text{MEAN}}(t)$. The classical loss is thus calculated according to

$$W_{\text{class}} = \frac{\sigma e^2}{12} \int_0^T \left(\frac{dB_{\text{MEAN}}}{dt} \right)^2 dt \quad (6)$$

111 It is found that ignoring the skin effect brings about a large overestimation of the loss above about $f =$
 112 400 Hz, for the considered $B_{\text{MEAN}}(t)$ peak value of 0.5 T considered in Fig. 5. An example of calculated
 113 induction profile $B(x, t_0)$ across the lamination thickness at a given instant of time t_0 is shown in Fig. 6.

114 It refers to $f = 1$ kHz and a time t_0 corresponding to the average flux density $B_{\text{MEAN}}(t_0) = 0$. Again, the
115 full and simplified DPMs predict very close results.

116 **IV. CONCLUSIONS**

117 In this work we have discussed a novel dynamic model for energy losses and hysteresis loops in soft
118 magnetic laminations based on simplified treatment of the Dynamic Preisach Model (DPM). It is
119 applied on experiments performed up to the kHz range in Fe-Si sheets, in the presence of substantial
120 skin effect, showing good agreement both with the experimental results and the prediction made using
121 the full machinery of the DPM. A remarkable advantage in computing time, which is reduced by a
122 factor around 60, is obtained substituting the full DPM with the present model.

123

124 **References**

- 125 [1] L.R. Dupre, O. Bottauscio, M. Chiampi, M. Repetto, and J. Melkebeek, *IEEE Trans. Magn.*, vol.
126 35, no. 5, pp. 4171-4184, 1999.
- 127 [2] S.E. Zirka, Y.I. Moroz, P. Marketos, and A.J. Moses, *Physica B: Condensed Matter*, vol. 343, no.
128 1, pp. 90-95, 2004.
- 129 [3] O. Bottauscio, M. Chiampi, C. Ragusa, M. Repetto, in "Studies in Applied Electromagnetics and
130 Mechanics. Non-linear electromagnetic systems" (IOS Press, V. Kose and J. Sievert Editors, 1998)
131 pp.449-454.
- 132 [4] O. Bottauscio, M. Chiampi, C. Ragusa, *J. Magn. Magn. Mater.* vol. 290-291, pp. 1446-1449, 2005.
- 133 [5] V. Basso, G. Bertotti, O. Bottauscio, M. Chiampi, F. Fiorillo, M. Pasquale, and M. Repetto, *J.*
134 *Appl. Phys.* vol. 81 pp. 5606 – 5608, 1997.
- 135 [6] G. Bertotti, *Journal of applied physics*, vol. 69, no. 8, pp. 4608-4610, 1991.
- 136 [7] E. Dlala, A. Belahcen, and A. Arkkio, *IEEE Transactions on Magnetism*, vol. 43, no. 11, pp. 3969-
137 3975, 2007.
- 138

139 **Figure captions**

140 Fig. 1- Excess fields provided by the full DPM, Model 1, and Model 2, for a sinusoidal dynamic
141 field $H(t) = H_a(t) - H_{cl}(t)$ (frequency $f = 200$ Hz, field peak value $H_p = 100\text{A}\cdot\text{m}^{-1}$) and corresponding
142 irreversible polarization J_{irr} provided by the DPM in a 0.35 mm thick Fe-(3.2wt%)Si-(0.5wt%)Al
143 lamination (dynamic constant $k_d=350\text{ A}^{-1}\text{s}^{-1}\text{m}$).

144 Fig. 2 - Block diagram of the simplified constitutive law $J(H)$ of the material, using the Model 2 as a
145 link between the field H and the static field H_{stat} (computation of the local excess field).

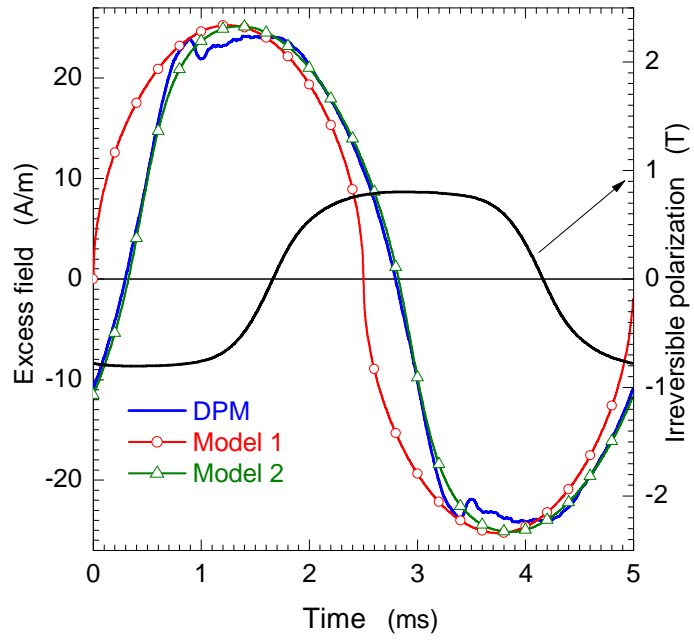
146 Fig. 3 - Example of the reconstructed $J(H)$ hysteresis loop with nested minor loops ($f = 200$ Hz, $H_p =$
147 $150\text{A}\cdot\text{m}^{-1}$)

148 Fig. 4 – Experimental and theoretical hysteresis loops at $f = 200$ Hz in the 0.35 mm thick Fe-
149 (3.2wt%)Si-(0.5wt%)Al lamination for sinusoidal induction ($B_p=0.5$ T). The measurements have been
150 performed on Epstein strips. Closed results are obtained by the full and the simplified DPM.

151 Fig. 5 – Same as Fig. 4 for the energy loss versus magnetizing frequency (DC – 2 kHz).

152 Fig. 6: Instantaneous induction profile $B(x,t_0)$ across the lamination thickness as obtained by the full
153 and the simplified (Model 2) DPM ($f = 1$ kHz, $-0.175\text{ mm} \leq x \leq 0.175\text{ mm}$). The time t_0 considered in
154 this figure is the one for which the mean flux density $B_{MEAN}(t_0) = 0$.

155



157

158

159

Fig. 1

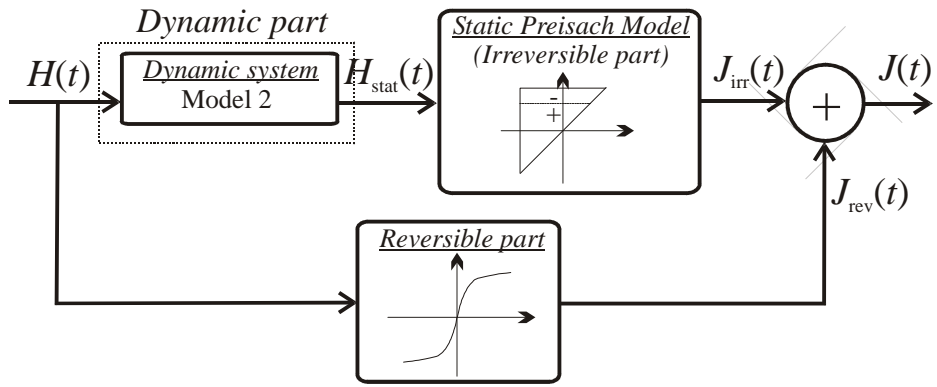


Fig. 2

160
161
162

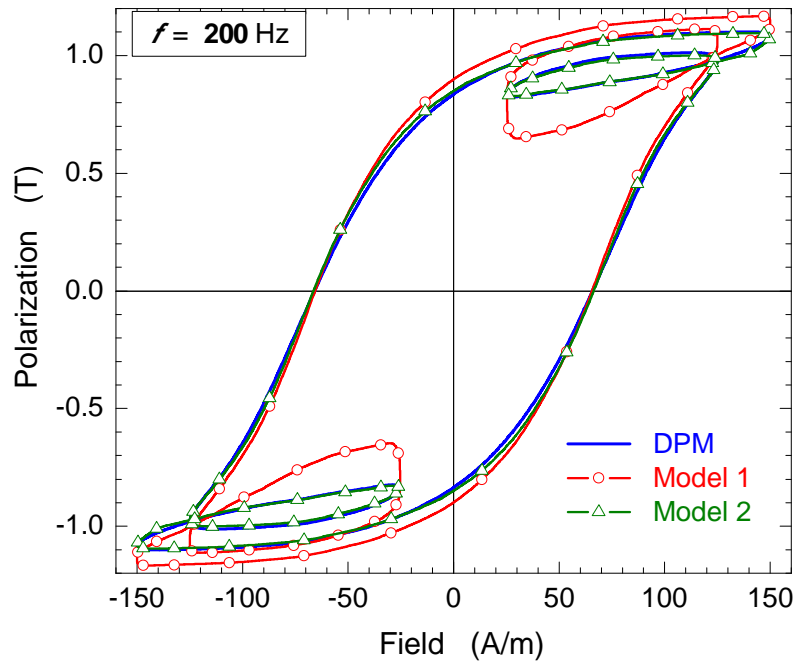


Fig. 3

163

164

165

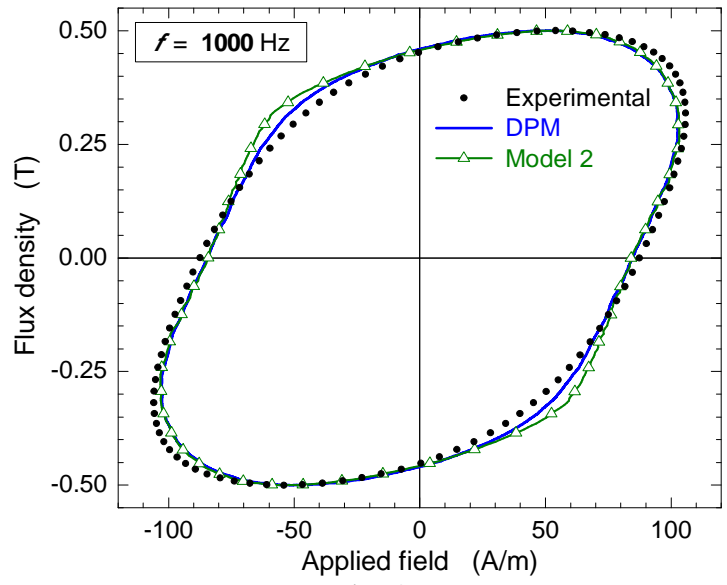


Fig. 4

166
167
168

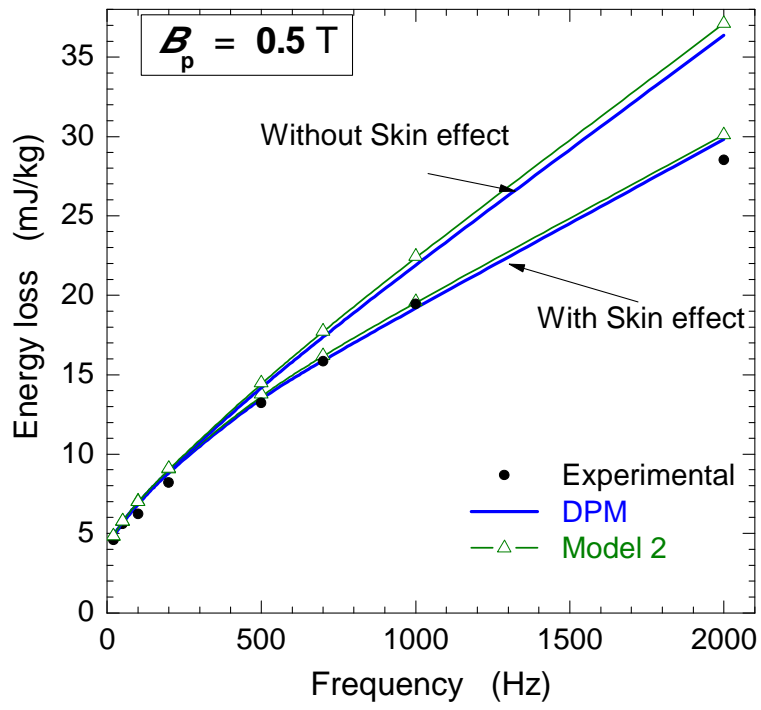
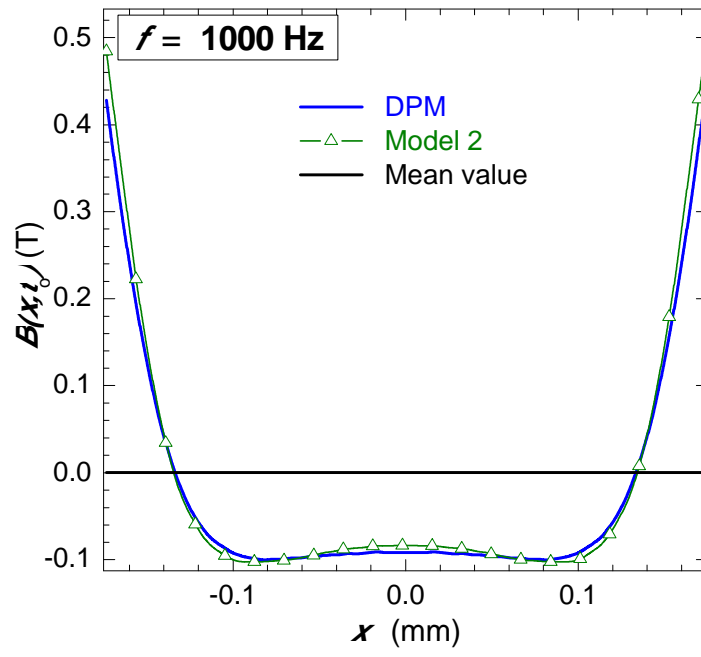


Fig. 5

169
170
171



172
173
174

Fig. 6